

# Finite difference modeling of the diffusive slow P-wave in poroelastic media

Shahin Moradi, Don C. Lawton, and Edward S. Krebes

## ABSTRACT

Biot's theory of poroelasticity predicts the presence of a slow P-wave in a fluid saturated medium due to the relative movement of the pore fluid with respect to the rock matrix. The slow P-wave, is highly diffusive in seismic frequencies and thus will not be observed in seismic data. However, in the case of zero fluid viscosity, this wave is a non-diffusive mode that travels through the medium. In this report both diffusive and non-diffusive modes are modeled using a previously developed finite-difference algorithm. It seems that in a uniform homogenous medium the amount of amplitude loss due to wave conversion in the diffusive case is very close to the one in the non-diffusive case. This shows that although the diffusive P-wave is not a traveling mode, it exists in the medium but dissipates quickly. The slow P-wave is particularly important where gas exists in the form of separate patches in the pore fluid. In those cases the wave conversions to the slow P-wave may dissipate a considerable amount of energy. Modeling wave propagation in such media is useful in monitoring studies for  $CO_2$  sequestration.

## INTRODUCTION

The study of the seismic wave behaviour in fluid saturated media is important in many geophysical applications. The reservoir rocks are known to be porous medium saturated with viscous fluids. As the seismic methods are extensively used to image the structure of the subsurface, understanding the wave phenomena has been always of interest for geophysicists.

Elastic wave propagation in a medium is governed by partial differential equations which could be numerically solved to simulate the wave traveling in that medium. Seismic wave modeling is a useful way of predicting the seismic data for a known geologic model, and is required for monitoring and planning purposes. For simplicity and also saving costs, the earth is usually assumed to be acoustic or elastic media. However, in reality, the reservoir rock are more complicated than a single elastic or acoustic phase. Maurice Biot first established theory of poroelasticity to describe wave propagating in a fluid saturated medium (Biot, 1962). Based on his theory, a poroelastic medium is composed of two phases. One phase is the porous elastic solid frame, and the other is the compressible viscous pore fluid. It is known that two compressional waves are generated in such medium. A fast P-wave due to the acceleration of the solid rock frame, and a slow P-wave due to the relative motion of the fluid with respect to the solid frame. In low frequencies the effect of fluid viscosity becomes stronger than the internal effects leading to diffusion of the slow mode. Therefore, the slow P-wave would not be observed as a traveling wave in seismic frequency. However, when the mobility factor  $b$  (the ratio of the fluid viscosity to the permeability) tends to zero, the slow mode starts to behave like a traveling wave. In either cases, the wave conversion to the slow mode causes energy loss in the medium that could be of interest in many geophysical applications.

Finite-difference method is a popular approach among all numerical methods of seismic modeling. There are several papers in the literature that have used finite-difference method for modeling wave propagation in the poroelastic media (Zhu and McMechan, 1991; Carcione and Quiroga-Goode, 1995; Zhang, 1999). For example, Zhu and McMechan (1991) used a standard finite-difference algorithm based on the displacements, and Dai et al. (1995) employed a MacCormack finite-difference scheme. Others implemented staggered-grid velocity-stress scheme for solving the wave equations (Zeng and Liu, 2001; Xiuming et al., 2003; Aldridge et al., 2004; Sheen et al., 2006). Furthermore, Zhang (1999) developed a quadrangle-grid velocity-stress finite-difference which was based on none-orthogonal grid. His scheme aimed to better handle the curved interfaces and surface topography.

A staggered-grid velocity-stress finite-difference algorithm similar to the one used by Sheen et al. (2006) was developed in an earlier work by the authors (Moradi et al., 2014). In this report, we add the effect of fluid viscosity to our developed algorithm to investigate the wave behaviour of the slow P-wave in the presence of the viscosity. It is expected that due to diffusion, the slow mode would not be detected as a traveling mode. However, the effect of diffusion should appear as a decrease in the amplitude of the fast P-wave due to the wave mode conversion.

## THEORY

Maurice Biot was the first to establish the theory of poroelasticity (Biot, 1962). He made the following assumptions to derive the equations of motion in the porous media: (1) the rock frame is assumed to be elastic and isotropic; (2) the pores are connected so that the fluid could travel through the pore space; (3) the seismic wavelength is much larger than the average pore size; and (4) the deformations are small enough that the mechanical processes become linear Biot (1962); Dai et al. (1995). The low frequency partial differential equations for isotropic poroelastic media can be written as first order equations in time:

$$\frac{\partial V_i}{\partial t} = A \frac{\partial \tau_{ij}}{\partial x_j} - B \left( \frac{\partial P}{\partial x_i} + b W_i \right) \quad (1)$$

$$\frac{\partial W_i}{\partial t} = B \frac{\partial \tau_{ij}}{\partial x_j} + C \left( \frac{\partial P}{\partial x_i} + b W_i \right) \quad (2)$$

$$\frac{\partial P}{\partial t} = -\alpha M \frac{\partial e_{kk}}{\partial t} - M \frac{\partial \varepsilon_{kk}}{\partial t} \quad (3)$$

$$\frac{\partial \tau_{ij}}{\partial t} = 2\mu \frac{\partial e_{ij}}{\partial t} + \left( \lambda_c \frac{\partial e_{kk}}{\partial t} + \alpha M \frac{\partial \varepsilon_{kk}}{\partial t} \right) \delta_{ij} \quad (4)$$

Where all symbols are defined in Table 1. In the 2D case, Equations 1 to 4 make a set of 8 coupled equations that could be used for numerical modelling (Equations 5 to 12 in Appendix). As previously mentioned, in an earlier work we developed a finite difference program in MATLAB to simulate the wave propagation in poroelastic media. The algorithm was based on a velocity-stress staggered grid method in the time domain. The PML method was also employed in order to eliminate the artifacts caused by the computational boundaries. For this purpose the grid was divided into two regions: the internal region,

where Equations 5 to 12 were solved; and the PML region, where some damping factors were added to the equations to dissipate outgoing waves efficiently. However in the previous work the algorithm was developed for the no-loss case, in which the viscosity of the fluid was assumed to be zero. The fluid viscosity has a direct effect on the mobility constant  $b$  which is the ratio of viscosity to permeability. In no-loss poroelastic medium the mobility factor  $b$  is zero and therefore the last terms in Equations 1 to 2 vanish. These terms describe the effect of fluid in the poroelastic medium and the behaviour of the slow mode. In seismic frequencies, the fluid effects become stronger than the internal effects, therefore the slow P-wave is diffusive and dies quickly in the medium. On the contrary, in the case where  $b = 0$ , the internal effects dominate over the fluid effect and the slow P-wave travels through the medium without diffusion. Carcione and Quiroga-Goode (1995) were the first who modeled the slow P-wave in low frequency range. They also showed that this mode makes the finite difference algorithm unstable numerically. However in our examples in this report the problem is stable and we do not focus on the stability issues.

## NUMERICAL EXAMPLES AND DISCUSSION

The numerical model used here is based on the well log data from the Quest Carbon Capture and storage project. The purpose of the Quest project is to store  $CO_2$  in the Basal Cambrian Sandstone, which is a saline aquifer within the Western Canadian Sedimentary Basin (WCSB). The log data and the numerical model generated based on this data were explained in detail in the previous work by the authors (Moradi et al., 2014; Moradi and Lawton, 2012). In this report we use a uniform homogenous model with the properties of the target injection formation, BCS, after injecting  $CO_2$ . The properties of this model are listed in Table 2. The pore fluid is assumed to be a mixture of 40%  $CO_2$  and 60% brine, and some of these properties were calculated using Gassmann's fluid substitution modeling.

As previously mentioned a finite-difference staggered grid algorithm was developed in MATLAB to model the wave propagation in poroelastic medium based on the Biot's theory. However in that study the effect of the fluid viscosity was ignored and the wave propagation in a no-loss poroelastic medium was modeled. In this report we include the fluid viscosity in the algorithm and show the changes caused by this term in the wave behaviour.

The unknowns in the partial differential equations are the particle velocities of the solid and the fluid, the stresses and also the fluid pressure. Particle velocities of the solid and the fluid were calculated for the model in Table 2. Three different values of the mobility  $b$  were used in the calculations. These values were chosen so that the algorithm shows the effect of the mobility constant on the slow wave mode. One of the values of  $b$  was the estimated value for the target formation (BCS) based on the pore fluid viscosity and the permeability of the BCS. The BCS is known to have a permeability of 1  $mD$  to  $> 1 D$ . The viscosity of the fluid was also estimated based on the viscosity of the  $CO_2$  and brine in the temperature and pressure at the depth of BCS (Moradi and Lawton, 2012). The average viscosity for the mixture of brine and  $CO_2$  is approximately  $10^{-5} kg/ms$ . We also assumed that the permeability of the porous rock is 1 $D$ . Therefore, the estimated value of  $b$  for our model is  $10^7 Pa sm^{-2}$ . In the cases of higher viscosity or lower permeability, the value of  $b$  increases. The issue with larger values of mobility is the stability of the finite difference algorithm. We have noticed that the larger the value of  $b$ , the more unstable the

Table 1. List of symbols and their definitions

| symbol             | discription  | formula  |
|--------------------|--|--|
| $e_{ij}$           | solid strain   | $\frac{1}{2} \left( \frac{\partial u_i}{\partial x_j} + \frac{\partial u_j}{\partial x_i} \right)$ |
| $\tau_{ij}$        | solid stress tensor                                  |  |
| $\vec{u}$          | particle displacement of the solid                   |  |
| $\vec{U}$          | particle displacement of the fluid                   |  |
| $\varepsilon_{kk}$ | $\nabla \cdot (\vec{u} - \vec{U})$                   |  |
| $\mu$              | shear modulus of the rock                            |  |
| $\lambda_c$        | Lame parameter of the saturated rock                 |  |
| $\alpha$           | Biot's coefficient                                   | $\left( 1 - \frac{K_{Dry}}{K_{Solid}} \right)$   |
| $K_{Solid}$        | bulk modulus of the solid                            |  |
| $K_{Dry}$          | bulk modulus of the dry rock frame                   |  |
| $K_f$              | bulk modulus of the fluid                            |  |
| $M$                | coupling modulus                                     |  |
| $P$                | fluid pressure                                       |  |
| $V_i$              | particle velocity of the solid                       | $\partial u_i / \partial t$  |
| $W_i$              | particle velocity of the fluid relative to the solid | $\partial (U_i - u_i) / \partial t$  |
| $\rho_f$           | density of the fluid                                 |  |
| $\rho_s$           | density of the solid                                 |  |
| $\rho$             | density of the saturated rock                        | $\phi \rho_f + (1 - \phi) \rho_s$  |
| $\phi$             | porosity   |  |
| $m$                | the fluid effective density                          | $T \rho_f / \phi$  |
| $T$                | tortuosity   |  |
| $b$                | fluid mobility                                       | $\eta / \kappa$  |
| $\kappa$           | permeability   |  |
| $\eta$             | fluid viscosity                                      |  |
| A                  |  | $\left( \frac{m}{m\rho - \rho_f^2} \right)$  |
| B                  | Coefficients defined in this paper for simplicity    | $\left( \frac{-\rho_f}{m\rho - \rho_f^2} \right)$  |
| C                  |  | $\left( \frac{-\rho}{m\rho - \rho_f^2} \right)$  |

algorithm becomes. Hence, the permeability of  $1D$  was assumed in this study to avoid unstable results.

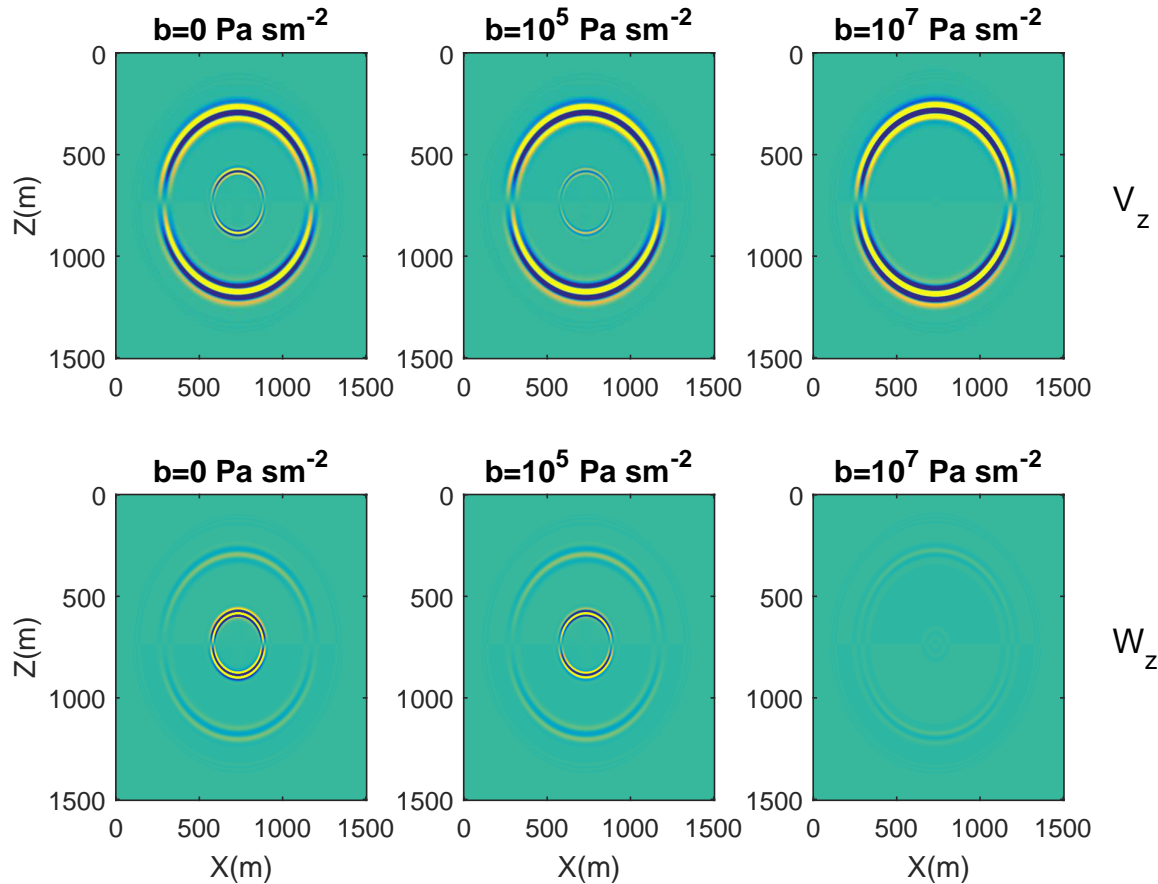


FIG. 1. Vertical particle velocities of the solid (top) and the fluid (bottom) for three different values of mobility  $b$ . By increasing the value of  $b$ , the slow P-wave start to become diffusive in the medium.

Figure 1 shows sample snapshots of the vertical particle velocities of the fluid ( $W_x$ ) and the solid ( $V_x$ ) at the time of 0.14 seconds. Two images on the left (top and bottom) correspond to the model with the mobility of zero. As expected, in the seismic frequency, for  $b = 0$  the slow P-wave is a traveling wave while for none-zero values of  $b$ , it is diffusive. For the case with  $b = 10^5 Pa sm^{-2}$  which are the two images in the middle (top and bottom), the slow P-wave seems weaker than the case with  $b = 0$ . Therefore, the larger  $b$  value, the more diffusive the slow mode becomes. In the case of  $b = 10^7 Pa sm^{-2}$  the slow P-wave does not exist in this time because it had been attenuated due to the fluid effect. Another point that worth mentioning is that in the fluid snapshots (three images on the bottom), the slow P-wave is larger in amplitude compared to the fast P-wave, which is probably because this wave is originated from the fluid movement.

In order to see the dissipation of the slow mode more clearly, some traces from the solid snapshots in Figure 1 are shown in Figure 2. In fact these traces are recorded by receivers in different distances from the source to represent a wave traveling in 1D case. These traces are calculated for two cases of  $b = 0$  and  $b = 10^5 Pa sm^{-2}$ . Since  $10^5 Pa sm^{-2}$  is not

considered as a large value for mobility, the slow P-wave is still detected. However, due to diffusion, the slow P-wave does not last long. By comparing these two traces we see that when  $b = 0$ , the slow P-wave does not dissipate when traveling through medium. In contrast, in the case of nonzero  $b$ , the slow P-wave dies quickly after a relatively short time. This figure not only shows the diffusion of the slow P-wave in seismic frequencies, but also the fact that the Biot's theory ignores the loss mechanism caused by the solid frame. It is clear that in absence of fluid viscosity ( $b = 0$ ) neither the fast nor the slow P-waves go through any attenuation. This is because the Biot's theory assumes the solid rock frame is purely elastic. However, this theory could be extended to the poro-viscoelastic case by adding memory variables to the partial differential equations (Carcione, 1998). The attenuation in P-wave could be then defined based on the White's model (White, 1975) to take the loss mechanism caused by the matrix-fluid interactions into account. This is accomplished by changing the coupling modulus  $M$  to relaxation function with dependency on time.

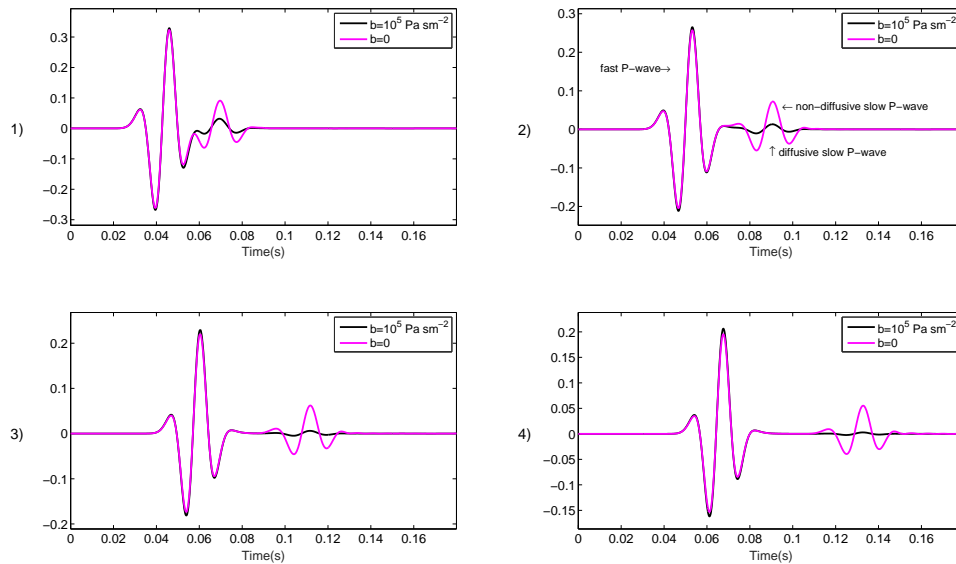


FIG. 2. Traces from the vertical particle velocities of the solid in poroelastic media for two values of  $b = 0$  and  $b = 10^5 Pa sm^{-2}$ . The slow P-wave in the case of non-zero mobility dissipates quickly while in the case of zero mobility does not change through time.

In Figure 3 we compare the trace generated by an elastic algorithm with the ones generated in the poroelastic algorithm with two values of  $b = 0$  and  $b = 10^5 Pa sm^{-2}$ . There is a considerable difference between the fast P-waves in the elastic and poroelastic cases. This is due to the wave conversion to the slow mode in the poroelastic medium. However, in the poroelastic traces, there is not a noticeable difference between the case with zero mobility and the one with nonzero mobility. This means that although the slow P-wave is not noticed as a traveling wave in seismic frequency, it does exist and leads to loss of energy in the poroelastic medium. It should be noted that these results are from a uniform homogenous model. In a layered media or a medium with patches of gas or fluid, more energy would dissipate through conversions to slow mode. As Shapiro and Müller (1999) showed, the amount of dissipated energy in these cases could be significant even in seismic

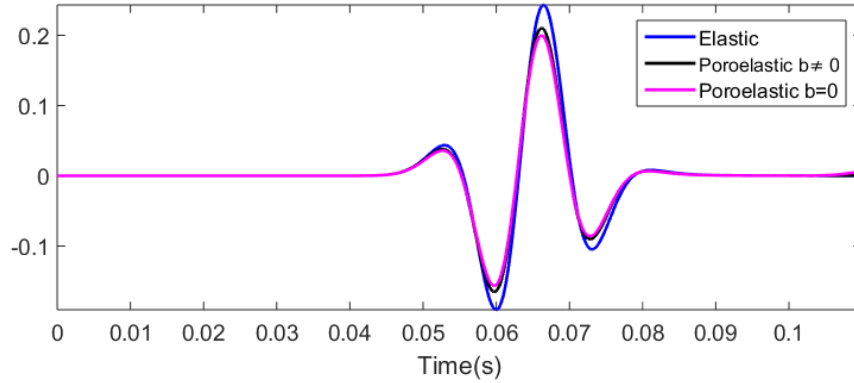


FIG. 3. Traces from an elastic algorithm are compared with the ones from poroelastic case with zero and non-zero mobility values. Due to conversion to the slow P-wave, the fast P-wave in the poroelastic case is smaller in magnitude compared to the elastic one.

frequency range.

### CONCLUSIONS

The fluid mobility constant was added to a previously developed finite-difference modeling program to simulate the wave propagation in poroelastic media. In seismic frequencies the slow P-wave is a diffusive wave and is not observed as a traveling mode unless the mobility parameter is zero. In this work we showed that although the diffusive slow wave is not a traveling mode wave, it causes energy loss that is due to conversion of the fast P-wave to slow P-wave. It is known that in finely layered poroelastic media, or in a rock saturated with fluid and patches of gas, the mode conversions could cause a significant loss in the seismic data. This algorithm could be used for modeling sequestration of  $CO_2$ , and any other cases in which the fluid saturation changes through time.

Table 2. Physical properties of the model used in this report

| Property    | The model   |
|-------------|---|
| $\rho_s$    | $2650 \text{ kg/m}^3$   |
| $\rho_f$    | $937 \text{ kg/m}^3$  |
| $K_{solid}$ | $38.00 \times 10^9 \text{ Pa}$  |
| $K_f$       | $0.25 \times 10^9 \text{ Pa}$   |
| $V_P$       | $3800 \text{ m/s}$  |
| $V_S$       | $2410 \text{ m/s}$  |
| $\phi$      | $16\%$  |
| $b$         | <i>zero</i><br>$10^5 \text{ Pa sm}^{-2}$<br>$10^7 \text{ Pa sm}^{-2}$ |

## ACKNOWLEDGMENTS

This research has been supported by the CREWES sponsors, Carbon Management Canada (CMC), and Natural Science and Engineering Research Council of Canada (NSERC) through the grant CRDPJ 379744-08. We thank Shell Canada Limited for providing the well data.

### Appendix: Biot's equations for the 2D case

The Equations 1 to 4, in the 2D case become:

$$\frac{\partial V_z}{\partial t} = A\left(\frac{\partial \tau_{zx}}{\partial x} + \frac{\partial \tau_{zz}}{\partial z}\right) - B\left(\frac{\partial P}{\partial z} + b W_z\right) \quad (5)$$

$$\frac{\partial V_x}{\partial t} = A\left(\frac{\partial \tau_{xx}}{\partial x} + \frac{\partial \tau_{xz}}{\partial z}\right) - B\left(\frac{\partial P}{\partial x} + b W_x\right) \quad (6)$$

$$\frac{\partial W_z}{\partial t} = B\left(\frac{\partial \tau_{zx}}{\partial x} + \frac{\partial \tau_{zz}}{\partial z}\right) + C\left(\frac{\partial P}{\partial z} + b W_z\right) \quad (7)$$

$$\frac{\partial W_x}{\partial t} = B\left(\frac{\partial \tau_{xx}}{\partial x} + \frac{\partial \tau_{xz}}{\partial z}\right) + C\left(\frac{\partial P}{\partial x} + b W_x\right) \quad (8)$$

$$\frac{\partial P}{\partial t} = -\alpha M\left(\frac{\partial V_x}{\partial x} + \frac{\partial V_z}{\partial z}\right) - M\left(\frac{\partial W_x}{\partial x} + \frac{\partial W_z}{\partial z}\right) \quad (9)$$

$$\frac{\partial \tau_{xx}}{\partial t} = (2\mu + \lambda_c)\frac{\partial V_x}{\partial x} + \lambda_c\frac{\partial V_z}{\partial z} + \alpha M\left(\frac{\partial W_x}{\partial x} + \frac{\partial W_z}{\partial z}\right) \quad (10)$$

$$\frac{\partial \tau_{zz}}{\partial t} = (2\mu + \lambda_c)\frac{\partial V_z}{\partial z} + \lambda_c\frac{\partial V_x}{\partial x} + \alpha M\left(\frac{\partial W_x}{\partial x} + \frac{\partial W_z}{\partial z}\right) \quad (11)$$

$$\frac{\partial \tau_{xz}}{\partial t} = \mu\left(\frac{\partial V_z}{\partial x} + \frac{\partial V_x}{\partial z}\right) \quad (12)$$

Note that  $\tau_{zx} = \tau_{xz}$ .

## REFERENCES

- Aldridge, D. F., Bartel, L., and Symons, N., 2004, Velocity-stress-pressure algorithm for 3d poroelastic wave propagation: 74th Ann. Internat. Mtg., Soc. Expl. Geophys., Expanded Abstracts, 1917–1920.
- Biot, M. A., 1962, Mechanics of deformation and acoustic propagation in porous media: *Journal of Applied Physics*, **33**, 1482–1498.
- Carcione, J. M., 1998, Viscoelastic effective rheologies for modelling wave propagation in porous media: *Geophysical Prospecting*, **46**, 249–270.
- Carcione, J. M., and Quiroga-Goode, G., 1995, Some aspects of the physics and numerical modeling of biot compressional waves: *J. Comp. Acous.*, **3**, 261–280.
- Dai, N., Vafidis, A., and Kanasewich, E., 1995, Wave propagation in heterogeneous, porous media: a velocity-stress, finite-difference method: *Geophysics*, **60**, 327–340.

- Moradi, S., Krebs, E. S., and Lawton, D. C., 2014, Time-lapse poroelastic modelling for a carbon capture and storage (ccs) project in alberta: CREWES Research Report, **25**.
- Moradi, S., and Lawton, D. C., 2012, Time lapse seismic monitoring of co2 sequestration at quest ccs project: CREWES Research Report, **24**.
- Shapiro, S. A., and Müller, T. M., 1999, Seismic signatures of permeability in heterogeneous porous media: Short note: *Geophysics*, **64**, No. 1, 99–103.
- Sheen, D. H., Tuncay, K., Baag, C., and Ortoleva, P., 2006, Parallel implementation of a velocity-stress staggered-grid finite-difference method for 2-d poroelastic wave propagation: *Computers and Geosciences*, **32**, 1182–1191.
- White, J. E., 1975, Computed seismic speeds and attenuation in rocks with partial gas saturation: *Geophysics*, **40**, 224–232.
- Xiuming, W., Hailan, Z., and Dong, W., 2003, Modelling seismic wave propagation in heterogeneous poroelastic media using a high-order staggered finite-difference method: *Chinese J. of Geophysics*, **46**, No. 6.
- Zeng, Y., and Liu, Q., 2001, The application of the perfectly matched layer in numerical modeling of wave propagation in poroelastic media: *Geophysics*, **66**, No. 4, 1258–1266.
- Zhang, J., 1999, Quadrangle-grid velocity–stress finite difference method for poroelastic wave equations: *Geophys. J. Int.*, **139**, 171–182.
- Zhu, X., and McMechan, A., 1991, Numerical simulation of seismic responses of poroelastic reservoirs using biot’s theory: *Geophysics*, **56**, No. 3, 328–339.